Molecular Crystals and Liquid Crystals

Publication details, including instructions for authors and subscription information:
http://www.tandfonline.com/loi/gmcl20

Erasing Strategies for Asymmetric Antiferroelectric Liquid Crystal Driving Schemes

P. L. Castillo [a], N. Bennis [a], M. Geday [a], X. Quintana [a], J. M. Otón [a], F. Beunis [b], K. Neyts [b] & V. Urruchi [c]

[a] Dpt. Tecnología Fotónica, ETSI Telecomunicación, Universidad Politécnica de Madrid, Ciudad Universitaria, Madrid, Spain

[b] Liquid Crystals & Photonics Group, Department of Electronics and Information Systems, Ghent University, Gent, Belgium

[c] Dpt. Tecnología Electrónica, E.P.S., Universidad Carlos III, Butarque, Leganés, Spain

Version of record first published: 31 Aug 2006

To cite this article: P. L. Castillo, N. Bennis, M. Geday, X. Quintana, J. M. Otón, F. Beunis, K. Neyts & V. Urruchi (2006): Erasing Strategies for Asymmetric Antiferroelectric Liquid Crystal Driving Schemes, Molecular Crystals and Liquid Crystals, 450:1, 39/[239]-53/[253]

To link to this article: http://dx.doi.org/10.1080/15421400600587670

Mol. Cryst. Liq. Cryst., Vol. 450, pp. 39/[239]–53/[253], 2006

ISSN: 1542-1406 print/1563-5287 online
DOI: 10.1080/15421400600587670

Erasing Strategies for Asymmetric Antiferroelectric Liquid Crystal Driving Schemes

P. L. Castillo
N. Bennis
M. Geday
X. Quintana
J. M. Otón
Dpt. Tecnología Fotónica, ETSI Telecomunicación, Universidad Politécnica de Madrid, Ciudad Universitaria, Madrid, Spain

F. Beunis
K. Neyts
Liquid Crystals & Photonics Group, Department of Electronics and Information Systems, Ghent University, Gent, Belgium

V. Urruchi
Dpt. Tecnología Electrónica, E.P.S., Universidad Carlos III, Butarque, Leganés, Spain

Antiferroelectric liquid crystals may be used for preparing high definition passively multiplexed video rate displays. Nevertheless, driving schemes employed in these applications customarily require the use of high voltage (~40 V) addressing signals that produce side effects such as ion currents. The generation and distribution of ions affect liquid crystal behavior under external applied voltage. Previous studies found dependence between surface density of adsorbed positive ions and sample thickness. Regarding electrooptical response, ion accumulation interferes with molecular reorganization upon driving, and their slow diffusion jeopardizes gray level stability. As a consequence, several display inconveniences, like permanent image trailing contribute to decrease image quality. This problem becomes particularly serious in the case of antiferroelectric cells with asymmetric alignment, where hysteresis shift allows the use of biasless driving schemes. The manufacturing protocol employed in our laboratory for asymmetric cells includes

Authors are indebted to Prof. R. Dabrowski for providing some of the AFLC mixtures. Financial support from the EU Thematic Network SAMPA and the Spanish MCyT program TIC03-9212 is appreciated.

Address correspondence to J. M. Otón, Dpt. Tecnología Fotónica, ETSI Telecomunicación, Universidad Politécnica de Madrid, Ciudad Universitaria, E-28040 Madrid, Spain. E-mail: jmoton@etsit.upm.es

the use of non-stoichiometric silicon monoxide on one of the display glass plates and an aligning buffed polymer on the other plate. Electrooptical response was analyzed under two new ways of driving, all of them with a biasless stabilization period, and based on relaxation strategies. Main changes were introduced in the way of erasing memory. One of them decreases response time whereas the other reduces dynamic range and saturation voltage. Best results are obtained when ion control is reinforced by the use of SiO_2 barrier layers between the glass coated electrodes and the SiO_x and polymer alignment layers. Finally, a full waveform reversal has been proposed with the aim of decrease dynamic range even more although a 5% of the darkest graylevels is lost.

Keywords: antiferroelectric; driving scheme; ions; liquid crystal; relaxation; waveform

INTRODUCTION

Nematic liquid crystals are nowadays the usual choice for preparing a wide variety of devices from simple LCDs to highly sophisticated large-area video-rate displays. Advances in research and industrial manufacturing processes overcome difficulties related to resolution, size, and working temperature range [1–5]. Yet smectic antiferroelectric liquid crystals (AFLCs) may provide alternative solutions in specific areas such as microdisplays, where their hysteresis, fast response time and wide viewing angle can be exploited [6–11]. Hysteresis of these materials leads to multistability and so the possibility of using passively multiplexed driving schemes at video rate, yielding competitive cost/quality ratios as compared to nematic active matrix TFTs.

However, AFLC dynamic properties are seriously affected by alignment layers. AFLCs usually lack a nematic phase within their phase sequence; as a consequence most commercial polyimides are useless as alignment layers. Polyamides such as Nylon 6 [10] seem to be a better choice, although long term stability has not been fully achieved yet, and contrast ratio is an issue. Nylon coated AFLC cells have been successfully multiplexed with 55μs selection slots [12] (i.e., the slot time required for multiplexing an SVGA display at 60 Hz video rate in double scan mode) and 36 μs slots (SXGA displays at video rate) with selection amplitudes of about 35 V. However, the pretransitional effect limits the dynamic contrast of these displays to about 30:1.

One way to alleviate pretransitional effect is to induce a permanent shift in the hysteresis curve; this can be achieved by using dissimilar alignment layers on either glass plate [13–15]. Electrooptical studies of asymmetric AFLCs were carried out using Nylon 6 on one side and non-stoichiometric SiO_x on the other side. Remarkable contrast

improvements were found, along with a 1–2 V shift in the hysteresis cycle. Moreover, asymmetric responses allow the use of relatively simple multiplexed driving schemes that deploy full analogue grayscales with no holding (bias) voltage [14,15].

Asymmetric responses have been reported by other authors as well [16–19], using nematic liquid crystals in different configurations, many of them based on WO_3 layers. Asymmetry on switching is explained through different surface charge densities over LC interfaces being enhanced for positive polarization while inhibited for negative one. These differences are qualitatively explained in terms of drains and sources of protons and other positive ions through reactions of hydrolysis and tungsten bronze formation inside the tungsten trioxide layer. The concentration of positive charge can vary when the polarity of external voltage changes, whereas the concentration of negative ions OH^- is constant and not mobile. This asymmetric charge distribution for both polarities affects in different way the electric field within the liquid crystal so that it changes the cell threshold voltage for negative and positive polarizations.

Performance of asymmetric AFLC displays in video-rate applications critically depends on the stability of the multiplexed grayscale, which is determined by the generation, migration, and accumulation of ions upon multiplexing. The waveform applied for developing this grayscale plays a crucial role concerning dynamic properties control. The aim of this work is to study electrooptical behavior under dynamic (multiplexed) working conditions with three different waveforms, with the eventual purpose of controlling (or even taking advantage of) ion evolution to optimize the resulting contrast, response times, memory performance and grayscale.

EXPERIMENTAL

Experiments were carried out in 1.5 μm thick surface stabilized cells of CS-4001 (Chisso) and the experimental mixture W-204A4 (Military University of Warsaw). Test cells were made by spinning a commercial polyamide (Nylon 6) on one glass plate and evaporating a 75 Å layer of SiO_x (in some cases, WO_3) onto the other plate (Fig. 1).

Electrooptical characterization was done at two frequencies: 0.1 Hz (triangular waveform, quasistatic) and 60 Hz (dynamic, using simulated multiplexing schemes) at a working temperature of 35°C. The basic biasless multiplexing waveform (single, Fig. 2a) is made of a selection pulse, a 0 V bias period over the frame and a reset section consisting of a single well pulse that additionally performs DC-compensation [12,15]. Note that only one hysteresis lobe is used in the

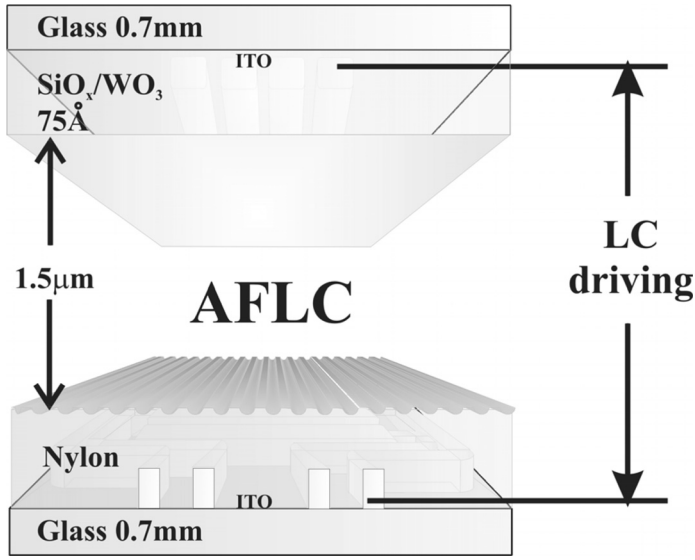

FIGURE 1 Cell assembling with asymmetric alignment configuration. Nylon 6 was distributed by spinning in one layer, and a semiconductor (either SiO_x or WO_3) by evaporation in the other layer. A SiO_2 barrier layer was optionally included between the electrodes and the alignment layers. Cells were filled with the AFLC CS4001 or the experimental mixture W-204A4.

driving scheme. The minimum slot duration (t_{slot}) was 110 μs in all cases. Grayscale was generated by subtracting slot-wide data pulses to selection and well pulses, and measured by integrating the resulting transmission curves over the whole frame.

Additionally, other waveform approaches were tested. A new reset section has been introduced: *double well* (Fig. 2b). Double well relaxation is made up of two well pulses of different amplitudes, the first being of higher voltage, and both pulses together DC-compensating the selection. A second new reset strategy has been developed: *ringlet* (Fig. 2c), with the aim of improving memory response of asymmetric cells. Ringlet consists of a sequence of high frequency AC pulses before the common DC-compensating well. Finally, a change of polarity has been introduced to decrease the dynamic range (DR) obtained with all the waveforms previously described. Time resolved transmission experiments have been done under multiplexing specifications, aiming to reproduce actual working conditions and to detect possible drifts arising from charge transport. Experiments were done as follows: the driving waveform was applied to the cell rows simulating multiplexing at the required frame rate, and data for gray levels were

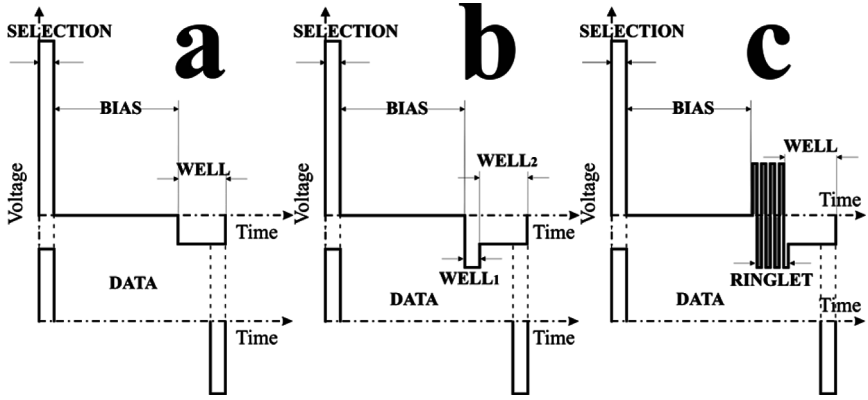

FIGURE 2 a) *Single well* waveform for multiplexed passive addressing of shifted AFLC cells. It is made up of a selection, a biasless period and a single well to DC compensate the selection. b) *Double well* waveform is made up of a selection, a biasless period and two wells for DC compensation. c) *Ringlet* waveform is made up of a selection, a biasless period and a sequence of high frequency AC pulses before a single well to DC-compensate the selection.

provided through the cell columns. Once any given gray level was selected, transmission was immediately recorded. In a separate measurement, the same gray levels were selected, and transmission was recorded after 25 s. The transmissions obtained in these two batches were compared to check gray level stability. To further account for memory effects, grayscales were generated in three different ways:

- Up: from dark state to saturation.
- Down: from saturation to dark state.
- Up-Down: an alternating sequence of gray levels starting on the clear and dark states and ending at the middle of the grayscale.

Additionally, a memory test consisting of a saturating frame followed by a number of dark level frames was performed on all the cells in order to study transmission evolution within consecutive frame times.

Negative and positive signs have been referred to the polymer side (nylon); therefore negative polarization is produced when a positive voltage is applied to the semiconductor side, either SiO_x or WO_3, and vice versa. With this sign convention, hysteresis cycles always shift towards negative voltages. In other words, the threshold voltage of the positive hysteresis lobe is lower than the threshold of the negative lobe. Consequently, the positive lobe (near-lobe) shall be the one

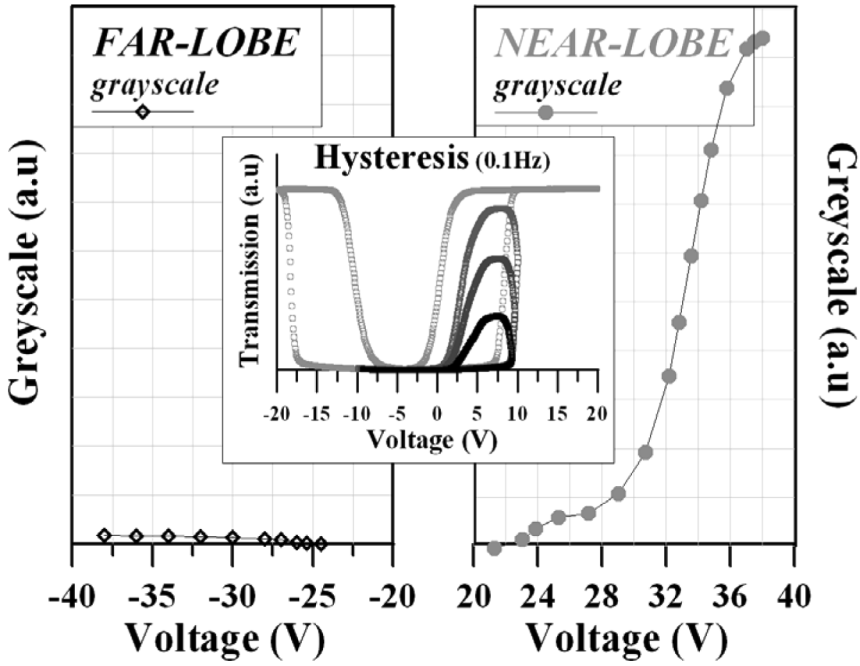

FIGURE 3 Near and far-lobe grayscales obtained with a single waveform of the same pulse width and amplitude but opposite polarity. The near-lobe grayscale has been completely developed whereas the far-lobe remains unswitched. Inset: Hysteresis cycles obtained with 1 Hz triangular AC pulses of different amplitudes.

used to generate the grayscale. The negative lobe (far-lobe) would remain unswitched if the same waveform with reversed polarization is applied (Fig. 3). As shown below, this feature can be employed to reshape the grayscale curve.

RESULTS AND DISCUSSION

Electrooptical Characteristics

As mentioned above, dynamic electrooptical response at video frequency of asymmetric cells shows a noticeable increase in contrast at 60 Hz (50–60%) as compared to the same AFLC response in symmetric cells. A typical 60 Hz-video-frequency grayscale curve from an asymmetric AFLC cell driven with single, double well and ringlet waveforms is shown in Figure 4(a–c). As seen in these pictures, grayscales show negligible changes when measured up, down or alternating

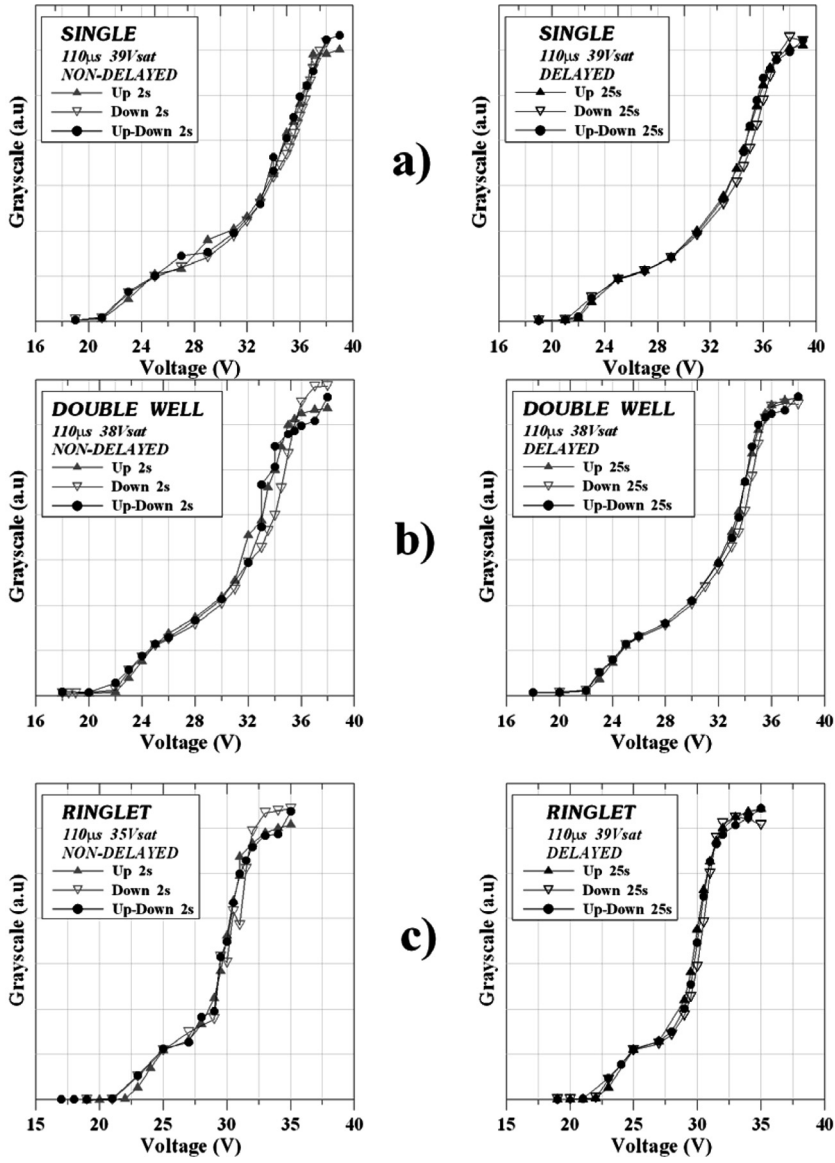

FIGURE 4 Grayscales developed from dark to bright, bright to dark and alternating bright-dark levels in single (a), double well (b), and ringlet (c) waveforms. No dependence on previous history of the pixel is found in either case. The left graph of every group has been acquired immediately after selecting the gray levels (acquisition time ~ 2 s). The right graphs have been acquired in a separate set of measurements; each point is taken after 25 s delay. No significant variations are noticed between non-delayed and delayed acquisitions.

up-down modes. Therefore, gray levels do not depend on the previous history of the pixel. The dark state (i.e. the dynamic threshold voltage) is similar in all three cases, while saturation is reached at different values. When single waveform is used, reaching the bright state requires a higher addressing voltage, thus widening the dynamic data range (DR) of the grayscale. This may be an issue in practical applications, since too wide a data range may preclude the use of standard CMOS electronics in the column drivers that generate data pulses.

Testing New Waveforms

High DR and other issues can improve when the new waveforms are employed. The most relevant electrooptic characteristics are shown in Table 1.

Analysis of these data indicates that there is a clear improve in the relaxation obtained when the double well is used. Rise and fall times are minimized by applying this relaxation scheme. In addition, DR decreases a 15% with respect to that obtained with single mode, while static and dynamic contrasts remain substantially constant. When the ringlet waveform is applied, DR is considerably reduced (38% of single mode value), and fall time decreases as well. Nevertheless, the main advantage of ringlet waveform concerns its memory behavior, as shown below.

The improved DR response obtained with these two driving schemes can be qualitatively related to ion shifts across the cell. It can be assumed in all cases that ions inside the LC reach their equilibrium position during the long biasless period (16 ms). However, a significant fraction of ions adsorbed onto the surface may still remain. The first well pulse of the double well scheme is a high voltage, short time pulse that contributes to the removal of such ions, bringing them back to the LC ion pool. Removed ions no longer contribute to the built-up internal field that opposes to switching. Note that the effect is shown for the highest voltage grey levels, i.e., those in which ion build-up is enhanced. This DR reduction is much more noticeable in the ringlet driving scheme. It can be derived that high frequency AC pulses are an efficient mechanism to remove adsorbed ions from the alignment layer.

Memory Tests

We have designed a procedure to test the memory effect of a liquid crystal embebed in a test cell with certain alignment layers. This "memory test" consists of one saturating frame followed by at least

TABLE 1 Waveforms Employed and Electrooptic Characteristics

CS-4001 SiO_x-Nylon			
Electrooptical measurements	Single	Double well	Ringlet
Selection [Voltage (V)/Width (μs)]	[39/110]	[38/110]	[35/110]
Bias [Voltage (V)/Length (μs)]	[0/16000]	[0/16000]	[0/16000]
Ringlet [Voltage (V)/Length (μs)]	–	–	[−20/27] (4 pairs)
$Well_1$ [Voltage (V)/Length (μs)]	–	[−3/110]	–
$Well_2$ [Voltage (V)/Length (μs)]	[−1.8/2383]	[−1.8/2120]	[−1.6/2406]
$D.R_{10–90\%}$ (V) Dynamic range	13	11	8
t_{rise} (μs)	20	15	20
t_{fall} (μs)	280	170	184
Contrast ratio (0.1 Hz)	89	89	89
Contrast ratio (60 Hz)	51	50	48

10 low transmission frames. Ideally, the dark state should be reached immediately after the first saturated frame. For applications using spatial color (color matrix or monochrome displays) at video rate, the cell is considered to pass the test, if no more than 4–5 frames are required for dark state to be completely achieved (eye integration smoothes the transition). On the contrary, sequential color driving schemes working at 180 Hz with R, G, B are required to display a full color picture at 60 Hz video frequency. In these applications, the desired gray level must be achieved in every frame, otherwise the residual transmission contaminates the next color frame and color saturation cannot be obtained. Sequential color provides higher resolution for it uses all pixels for every color; its drawback is that a much faster response is required.

Figure 5 shows the memory test obtained with single mode in CS-4001 asymmetric cells. The evolution of the transmission requires only two frames to be fully stabilized, being suitable for spatial – but not for sequential – color driving. This memory test was also applied to double well and ringlet waveforms; results with the main part of transmission evolution are depicted in Figure 6. Double well exhibits the same leakage transmission as single mode in the first dark frame after saturation. However, the ringlet waveform performs a nearly ideal memory test, being a good candidate for video rate sequential color applications.

Relaxation of gray levels to dark state is closely related to ion adsorption. Indeed, the internal field induced by adsorbed ions effectively acts as a bias voltage that stabilizes any gray level. The induced voltage is lower than the required bias for the gray levels to be kept;

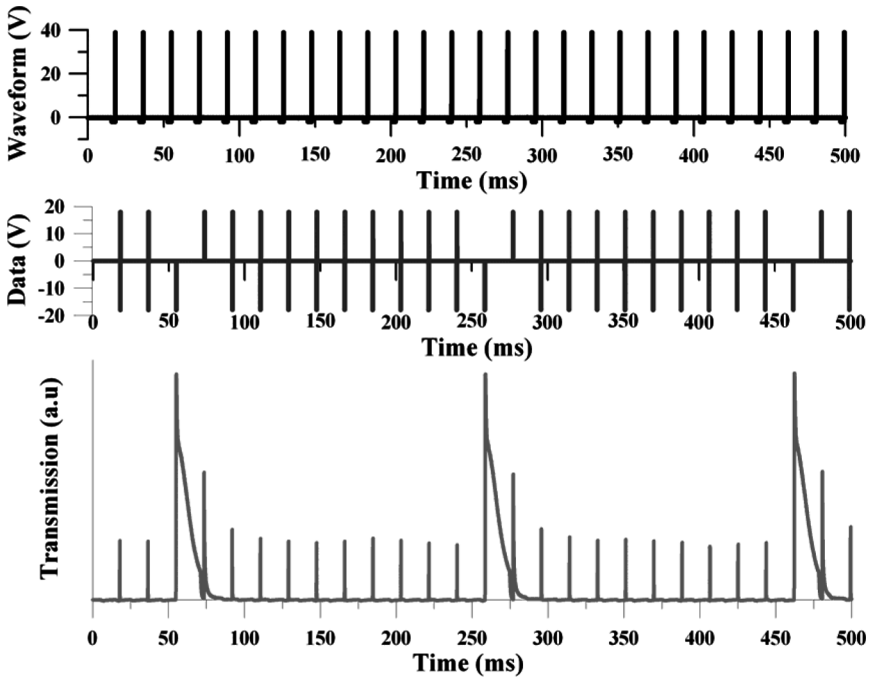

FIGURE 5 Memory test for a CS-4001 SiO_x-Nylon cell when the single scheme of relaxation is applied. Two sequences of the basic waveform (upper), data subtracted (medium) and transmission evolution (lower) are shown.

nevertheless, it contributes to slow down their relaxation. Again, the efficiency of high frequency AC pulses in removing adsorbed ions is demonstrated. Note that the time scale for gray level stabilization in memory tests is the same as the frametime. This short-term stabilization reached by ringlet schemes is crucial to lead asymmetric AFLC displays to video-rate practical applications.

Waveform Reversal

Concerning DR reduction, a new approach has been designed, namely waveform reversal. The shift introduced by asymmetric alignment in hysteresis curve, leads to dissimilar grayscales on the hysteresis lobes. The lobe closer to zero volts (*near-lobe*) is used to develop grayscales in biasless modes. The other lobe (*far-lobe*) develops its grayscale at higher voltage (Fig. 3). Therefore, if the polarity of a grayscale-generating waveform is inverted, the same driving scheme can be applied to

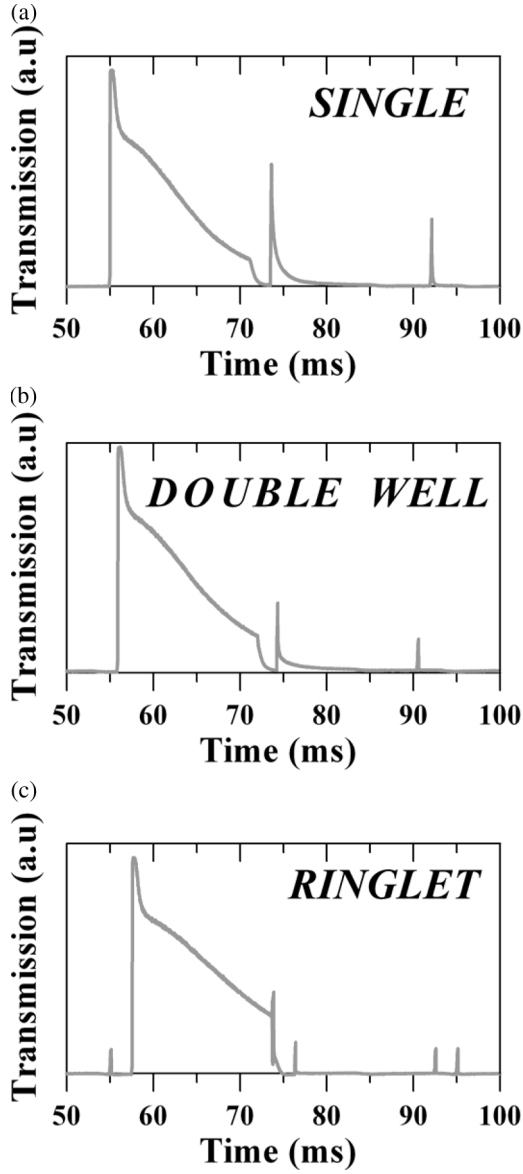

FIGURE 6 Evolution of the transmission for the first dark frame after saturation in single (a), double well (b), and ringlet (c) waveforms. The leakage transmission exhibited for single and double well precludes the possibility of sequential color driving whereas it is enhanced when ringlet waveform is applied.

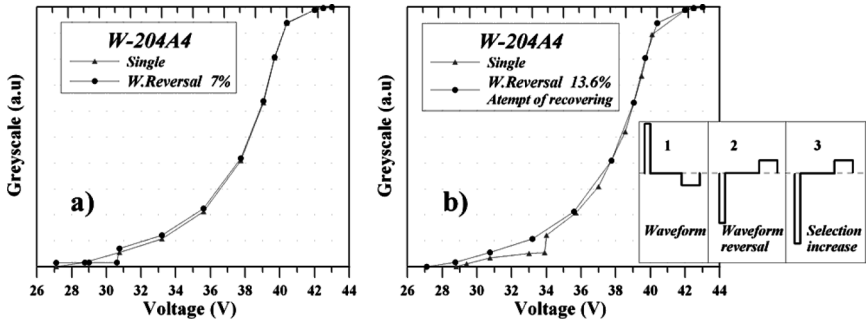

FIGURE 7 Waveform reversal carried out with single relaxation in W-204A4 asymmetric cells. The inversion point may be below 10% transmission (a) or above this limit (b). The graphic in b) shows also the result of an increase in voltage pulse for inverted waveform as an attempt of recovering the lost fraction of the grayscale.

the far-lobe leading to dark states. Besides reductions in DR, the advantage of this approach is that the effect on ion distribution is dramatic, the dark state being achieved in one single frame with no memory effect or trailing images.

Figure 7a shows an example of polarity inversion carried out with W-204A4 SiO_x asymmetric cells with single waveform. Waveform reversal effectively wipes out a fraction of the grayscale – the darkest gray levels. The specific point within the grayscale where inversion is applied is a tradeoff between the DR width and the grayscale integrity. In this example, the inversion point has been chosen in the 5–10% transmission levels. The grayscale was measured as usual from saturation to dark state (down) till effective voltage applied to the cell was in the final section of the near-lobe grayscale. Then, waveform and data polarity were reversed and the transmission fell down to the grayscale of the far-lobe region. As a consequence, the dark state is reached immediately and 0–100% DR is consequently reduced. However, as there is no way of connecting near and far lobe sections, the main drawback of this method is that the grayscale fraction between direct and reverse polarity is lost. An attempt of recovering this fraction was done in W-204A4 asymmetric cells by performing waveform reversal over the lowest 10% of the grayscale, and increasing at the same time the data voltage of the inverted selection pulse with the aim of connecting near and far lobe grayscales (Fig. 7b). Results show that full recovering is not possible, whereas reduction in 0–100% DR is negligible. Similar results are obtained with waveform reversals in the case of ringlet mode and CS-4001 liquid crystal (Fig. 8). Table 2

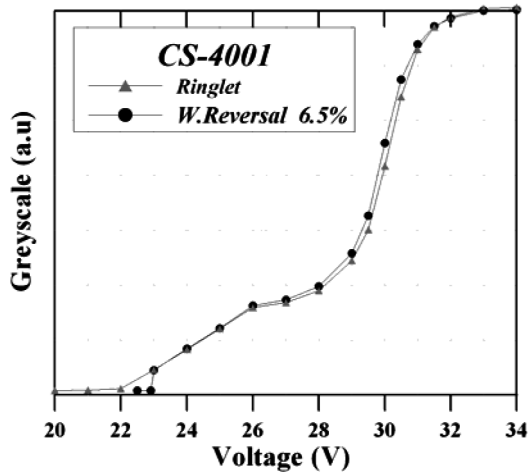

FIGURE 8 Waveform reversal carried out with ringlet way of relaxation in CS-4001 asymmetric cells under the 10% of the transmission. A decrease in DR 0–100% can be obtained whereas a 5–6% of the full grayscale without inversion is lost.

offers a summary of 10–90% and 0–100% DRs for all the cases studied in Figures 7a, 7b, and 8. The percentage of grayscale lost in the reversal is about 5–6% while DR reduction is about 20% in single-well and ringlet cases. The evolution of DR values is depicted in Figure 9. When waveform reversal is applied below the 10% transmission point, the 10–90% DR obviously remains constant, while the 0–100% DR decreases substantially

TABLE 2 Comparison of Grayscales with and without Polarization Reversal

	W-204A4		
AFLC Waveform	Single attempt of recovering	Single	CS-4001 Ringlet
NO W. Reversal			
$DR_{10–90\%}$ (V)	7.4	7.4	8.0
$DR_{0–100\%}$ (V)	15.9	15.9	14.0
Waveform Reversal (at x% in the grayscale)			
$DR_{10–90\%}$(V)	7.1 (at 13.6%)	7.4 (at 7.0%)	8.0 (at 6.5%)
$DR_{0–100\%}$ (V)	14.2 (at 13.6%)	12.4 (at 7.0%)	11.5 (at 6.5%)
% lost	6.6	5.4	5.3

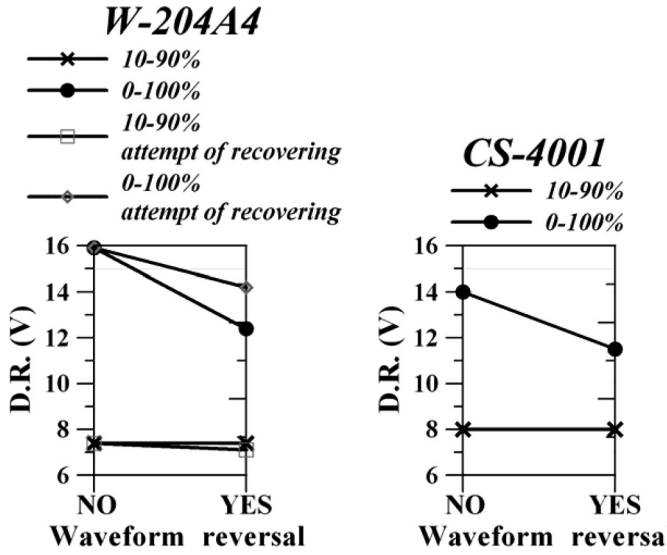

FIGURE 9 DR decrease when waveform reversal is applied to W-204A4 with single waveform (left) and CS-4001 with ringlet waveform (right).

CONCLUSIONS

Three different addressing schemes have been tested to characterize AFLC asymmetric cells: single, double well and ringlet. Electrooptical responses obtained show that single provides the best contrast, double well the lowest response times and ringlet decreases DR and saturation voltage. Improvements are associated to removal of adsorbed ions onto the alignment surface. A procedure to test memory behavior under video rate conditions for display applications has been proposed and applied to CS-4001 asymmetric cells with the three waveforms previously described. Video rate spatial color conditions are fulfilled by the three waveforms whereas only ringlet scheme has demonstrated to be adequate for sequential color requirements.

A strategy based on a full change of polarity for the waveform used has been applied at the beginning in the low part of the grayscale. As a consequence, a 20% decrease in 0–100% DR can be obtained with the drawback of losing about 5% of the darkest gray levels.

REFERENCES

[1] Dąbrowski, R. (2004). *Mol. Cryst. Liq. Cryst.*, *421*, 1.
[2] Wolinski, T. R., Dąbrowski, R., Bogumil, A., & Stolarz, Z. (1995). *Mol. Cryst. Liq. Cryst.*, *263*, 389.

[3] Castillo, P. L., Quintana, X., Otón, J. M., Dąbrowski, R., & Filipowicz, M. (2004). *Mol. Cryst. Liq. Cryst.*, *422*, 65.
[4] D'Have, K., Dahlgren, A., Rudquist, P., Lagerwall, J. P. F., Andersson, G., Matuszczyk, M., Lagerwall, S. T., Dąbrowski, R., & Drzewinski, W. (2000). *Ferroelectrics.*, *244*(1–4), 415.
[5] Uchida, T., Ishinabe, T., Nakayama, T., Suzuki, M., & Miyashita, T. (2004). *Jap. J. Appl. Phys.*, *43*(12), 8094.
[6] Abdulhalim, I. (2003). *J. Appl. Phys.*, *93*(8), 4930.
[7] Otón, J. M., Quintana, X., Castillo, P. L., Lara, A., Urruchi, V., & Bennis, N. (2004). *Opto-Electron. Rev.*, *12*(3), 263.
[8] Quintana, X., Castillo, P. L., Otón, J. M., Bennis, N., Lara, A., Urruchi, V., & Dąbrowski, R. (2004). *Opto-Electron. Rev.*, *12*(3), 291.
[9] Urruchi, V., Dąbrowski, R., Gayo, J. L., Otón, J. M., & Quintana, X. (2004). *Mol. Cryst. Liq. Cryst.*, *410*, 995.
[10] Bennis, N., Dąbrowski, R., Spadlo, A., Kula, P., Quintana, X., & Otón, J. M. (2004). *Mol. Cryst. Liq. Cryst.*, *422*, 37.
[11] Piecek, W., Raszewski, Z., Perkowski, P., Przedmojski, J., Kedzierski, J., Drzewinski, W., Dabrowski, R., & Zielinski, J. (2004). *Ferroelectrics.*, *310*, 269.
[12] Quintana, X., Gayo, J. L., Rodrigo, C., Urruchi, V., & Otón, J. M. (2000). *Ferroelectrics*, *246*, 211.
[13] Gayo, J. L., Otón, J. M., Quintana, X., Urruchi, V., Toscano, C., & Bennis, N. (2002). *Mol. Cryst. Liq. Cryst.*, *375*, 121.
[14] Gayo, J. L., Otón, J. M., Quintana, X., Urruchi, V., Toscano, C., & Bennis, N. (2002). *Mol. Cryst. Liq. Cryst.*, *375*, 121.
[15] Gayo, J. L., Quintana, X., Bennis, N., & Otón, J. M. (2004). *Mol. Cryst. Liq. Cryst.*, *410*, 451.
[16] Alexe-Ionescu, A., Ionescu, A., Scaramuzza, N., Strangi, G., & Versace, L. (2001). *Phys. Rev. E*, *64*, 011708.
[17] Bartolino, R., Scaramuzza, N., Lucchetta, G., Barna, E. S., Ionescu, A. Th., & Blinov, L. M. (1999). *J. Appl. Phys.*, *85*, 2870.
[18] Barbero, G., Zvezdin, A. K., & Evangelista, L. R. (1999). *Phys. Rev. E*, *59*(2), 1846.
[19] Pereira, H. A., Batlioto, F., & Evangelista, L. R. (2003). *Phys. Rev. E*, *68*(2), 040701.